Dual-Aptamer Modification Generates a Unique Interface for Highly Sensitive and Specific Electrochemical Detection of Tumor Cells

Liming Qu, Jinhai Xu, Xiaofang Tan, Zhuang Liu, Ligeng Xu,* and Rui Peng*

Institute of Functional Nano & Soft Materials (FUNSOM) & Collaborative Innovation Center of Suzhou Nano Science and Technology, Jiangsu Key Laboratory for Carbon-Based Functional Materials & Devices, Soochow University, Suzhou, Jiangsu 215123, China

S *Supporting Information*

ABSTRACT: Because circulating tumor cells (CTCs) have been proven to be an important clue of the tumor metastasis, their detection thus plays a pivotal role in the diagnosis and prognosis of cancer. Herein, we fabricate an electrochemical sensor by directly conjugating two cell-specific aptamers, TLS1c and TLS11a, which specifically recognize MEAR cancer cells, to the surface of a glassy carbon electrode (GCE) via the formation of amide bonds. The two aptamers are simultaneously conjugated to the GCE surface via precisely controlled linkers: TLS1c through a flexible linker (a single-stranded DNA T_{15}; ss-TLS1c) and TLS11a through a rigid linker (a double-stranded DNA T_{15}/A_{15}; ds-TLS11a). It is found that such ss-TLS1c/ds-TLS11a dual-modified GCEs show greatly improved sensitivity in comparison with those modified with a single type of aptamer alone or ds-TLS1c/ds-TLS11a with both rigid linkers, suggesting that our optimized, rationally designed electrode–aptamer biosensing interface may enable better recognition and thus more sensitive detection of tumor cells. Through the utilization of this dual-aptamer-modified GCE, as few as a single MEAR cell in 10^9 whole blood cells can be successfully detected with a linear range of 1–14 MEAR cells. Our work demonstrates a rather simple yet well-designed and ultrasensitive tumor cell detection method based on the cell-specific aptamer-modified GCE, showing a promising potential for further CTC-related clinical applications.

KEYWORDS: circulating tumor cells, cell-specific aptamer, biosensing interface, chemically modified electrode, electrochemical detection
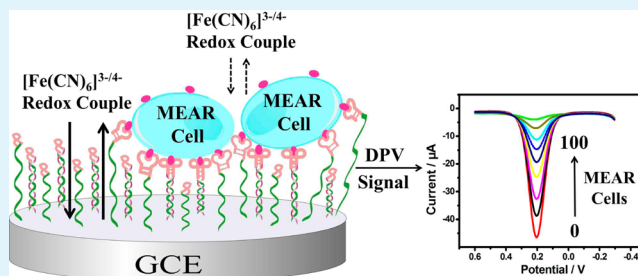
1. INTRODUCTION

Circulating tumor cells (CTCs) circulating in the peripheral blood or lymphatic vessels are originated from primary tumors or metastasis locus and could travel to distant tissue sites and then eventually form new tumor deposits.[1,2] Numerous studies have indicated that the number of CTCs in peripheral blood is positively related to the tumor metastasis and thus could serve as a valuable parameter in evaluating the therapeutic effects and predicting the survival of cancer patients.[3,4] Currently, Cellsearch based on immunomagnetic separation is the only FDA-approved CTC detection method.[5,6] In the meantime, tremendous efforts have been devoted by many different groups to develop new methods for the effective detection of CTCs in the past decades.[7-14] However, many of currently developed CTC detection techniques are generally costly, time-consuming, or need advanced instrumentation and not easy to implement.[15] The ideal CTC detection method should be extremely sensitive, specific, reproducible, simple, and user-friendly in clinical settings.[16-18]

Aptamers are short single-stranded (ss) nucleic acids that can recognize and interact with their targets with high specificity and affinity.[19,20] They provide significant advantages compared to antibodies, such as ease of preparation and modification and lack of immunogenicity.[21-23] Aptamer-based electrochemical

detection methods hold increasing promise and show many advantages such as rapid response, high sensitivity, good stability, and low cost.[24-29] In recent years, aptamer-based electrochemical biosensors used to detect tumor cells have also received significant attention.[30-33] These methods are mainly based on the high specificity and affinity of aptamers that interact with biomarkers on the cancer cell surface, such as graphene functionalized cyclic voltammetry (CV) aptasensor, aptamer-quantum dots cytosensor, and dual-aptamer probe for simultaneous electrochemical biosensor.[15,26,27,34-37] Although those methods have facilitated the CTC detection, they share certain limitations such as complex fabrication with multiple steps of modification.[26,38] To our best knowledge, the best detection limit based on the aptamer–electrochemical detection method has been reported to be hundreds of cancer cells per millimeter,[26,39] which obviously needs further optimization.

On the basis of the previous research, herein, we design a rather simple aptamer-based electrochemical detection method and realize ultrasensitive CTC detection in blood cells. BNL

1ME A.7R.1 (MEAR) cells, a liver cancer cell line originally derived from BALB/cJ mice, are used as a model to study the detection ability of aptamer fabricated electrochemical biosensor. Aptamers TLS1c and TLS11a, which specifically recognize the MEAR cells developed in previous studies,[40] are covalently coupled to the commercial glassy carbon electrode (GCE) with single-stranded (ss) T_{15} and double-stranded (ds) T_{15}/A_{15} linkers, respectively. Such a design would generate a favorable interface for better recognition of the cancer cells when they approaching the electrode surface. Compared to previously reported aptamer−electrochemical CTC detection methods, as well as other designs with GCE modified by a single aptamer (ds-TLS1c) or by dual-types of aptamers but with both rigid linkers (ds-TLS1c/ds-TLS11a), the ss-TLS1c/ds-TLS11a-modified electrode possesses the highest signal-to-noise ratio, and is able to detect a single MEAR cell within 10^9 whole blood cells (WBC). Our results highlight the utmost importance of nano−bio interfaces in optimizing the performance of biosensors, and suggest the great promise of this simple electrochemical method in early CTC detection.

2. EXPERIMENTAL SECTION

2.1. Materials and Cell Lines.
Amine modified aptamers K88 (specific for *Escherichia coli* K88, 5′-T_{15}GGCGACCCCCGGGCT-ACCAGACAATGTACGC-3′)[41] and TBA (specific for thrombin-5′-T_{15}GGTTGGTGTGGTTGG-3′),[42] amine, or fluorescein (FITC) modified aptamers TLS1c (5′-T_{15}ACAGGAGTGATGGTTGTTAT-CTGGCCTCAGAGGTTCTCGGGTGTGGTCACTCCTG-3′) and TLS11a (5′-T_{15}ACAGCATCCCCATGTGAACAATCGCATT-GTGATTGTTACGGTTTCCGCCTCATGGACGTGCTG-3′) that specifically bind to BNL 1ME A.7R.1 (MEAR) cells were synthesized by TaKaRa Co. Ltd (Dalian, China). 2-Amino-2-(hydroxymethyl)-1,3-propanediol (Tris), hydrochloric acid, ethylene diamine tetraacetic acid (EDTA), 1-ethyl-3-(3-(dimethylamino)propyl) carbodiimide (EDC), *N*-hydroxysuccinimide (NHS), potassium hexacyanoferrate, potassium ferricyanide, potassium chloride, nitric acid, and potassium dichromate were purchased from Sigma-Aldrich. Two mammalian tumor cell lines, MEAR and HeLa, were grown in a 5% CO_2 incubator at 37°C in Dulbecco's modified Eagle's medium (DMEM) supplemented with 10% fetal bovine serum (FBS), 100 μg/mL penicillin, and 100 μg/mL streptomycin.

2.2. Surface Modification of the Electrode.
Before surface modification, the GCE (CHI 104 glassy carbon disk working electrode, CH Instruments, Inc.) was precleaned by polishing with 0.3 and 0.05 μm alumina/water slurries until a mirror-like surface was obtained, followed by sonication and extensive washing using distilled water to remove alumina from the electrode surface.[43] The precleaned GCE was oxidized at +1.5 V for 60 s in an aqueous solution containing 2.5% $K_2Cr_2O_7$ and 10% HNO_3 as previously described,[44] and then soaked in 0.02 M phosphate buffered saline (PBS, pH 6.4) containing 0.03 M EDC and 0.01 M NHS at room temperature for 15 min. After removal of excess EDC and NHS, MEAR cell specific aptamers: 0.1 nmol ds-TLS1c, 0.05 nmol ds-TLS1c/0.05 nmol ds-TLS11a, 0.05 nmol ss-TLS1c/0.05 nmol ds-TLS11a, or 0.05 nmol ss-K88/0.05 nmol ds-TBA were applied to the GCE surface, respectively, and incubated at room temperature for 1 h. The unbound aptamers were then washed away using 0.02 M PBS buffer, collected, and the concentration determined using a NanoDrop 2000c UV−vis spectrophotometer (Thermo Scientific) to calculate the immobilization efficiency. About 70% of the aptamers were immobilized on the GCE surface (3 mm in diameter), giving an aptamer density of 0.01 ± 0.0002 nmol/mm². The aptamer-functionalized GCEs were then used for cancer cell detection. For aptamer density optimization experiments, 0.025 nmol ss-TLS1c/0.025 nmol ds-TLS11a and 0.1 nmol ss-TLS1c/0.1 nmol ds-TLS11a were used.

2.3. Aptamer-MEAR Binding Reactions.
The human blood samples were collected from 20 healthy volunteers (aged 22−45 years) according to approved local protocol. To minimize individual differences, the blood samples were mixed together and stored at 4 °C. Before detection, blood samples were diluted with equal volumes of PBS buffer (pH7.4) and WBC were carefully collected by centrifugation at 1200g for 15 min at 4 °C as previously described,[45] resuspended in PBS buffer (pH7.4), and counted. To minimize the effect of nonspecific binding during detection, aptamer-functionalized GCEs were first blocked by incubating with 10^9 WBC in 1 mL PBS buffer at 4 °C for 45 min. Binding reactions were then carried out by incubating the blocked electrode in 10^9 WBC (in 1 mL PBS buffer) containing desired numbers of MEAR or HeLa cells at 4 °C for 15 min before electrochemical analysis. To ensure accuracy, the exact number of cancer cells was counted under a microscope before addition into the WBC sample.

2.4. Electrochemical Measurements.
All electrochemical measurements including CV, differential pulse voltammetry (DPV), and electrochemical impedance spectroscopy (EIS) were performed using a CHI 660D electrochemical workstation (Shanghai CH Instruments, China). The electrode assembly consists of a platinum wire as the counter electrode, an Ag/AgCl electrode as the reference electrode, and a GCE as the working electrode. The measurement buffer contains 5 mM $[Fe(CN)_6]^{3−/4−}$ as the redox indicator. CV was recorded in the range from −0.3 to +0.6 V and at a scan rate of 0.1 V/s. DPV was recorded within the potential range from −0.4 to +0.8 V under a modulation amplitude of 50 mV and a scan rate of 4 mV/s. AC impedance spectra for GCE were recorded in the same measurement buffer in a frequency range of 0.01 to 100 Hz and AC amplitude of 5 mV.

3. RESULTS AND DISCUSSION

3.1. Design of the Dual-Aptamer-Modified Electrode.
To develop electrochemical sensors for CTC detection, we need to conjugate cancer-cell specific aptamers onto the surface of the electrode. However, surface-based biomolecular detection often sacrifices the accessibility of probe molecules on the interface to targets on the cell membrane owing to the lack of precise control of the spatial orientation and positioning of probe molecules on the surface.[46] To improve the recognition efficiency of probe molecules on the sensing interface for enhanced detection efficiency and sensitivity, it is thus important to optimize their conformation and packing density. Therefore, in our rationally designed system (Figure 1), two aptamers, TLS1c and TLS11a, which both specifically bound to MEAR cancer cells (Figure S1 in the Supporting Information), were simultaneously coupled to the GCE surface via different DNA linkers. While TLS11a was coupled to the GCE surface rigidly by a dsDNA linker (T_{15}/A_{15}), the other aptamer, TLS1c, was coupled to the electrode surface via ss-T_{15} linker. The rigid structure of dsDNA linker would have low binding to the graphite surface and can thus keep the TLS11a probe away from the electrode surface. Because ds-TLS11a and ss-TLS1c are mixed, the rigid dsDNA may also help prevent the laying down of ssDNA. Thus, the recognition of a MEAR cell by aptamers would occur away from the surface of the electrode, minimize the steric hindrance on the aptamer-cell recognition, and lower the background signal. On the other hand, the extended ssDNA linker with a much more flexible structure compared to rigid dsDNA linker enables ss-TLS1c to swing on the electrode surface with a certain freedom, allowing its effective binding to its targets (biomarkers on MEAR cells) and enhancing the detection efficiency.

Upon efficient recognition of the target cells, in our case, MEAR cells, the specific binding of the cells to the modified electrode would bring a dramatic steric hindrance effect on the
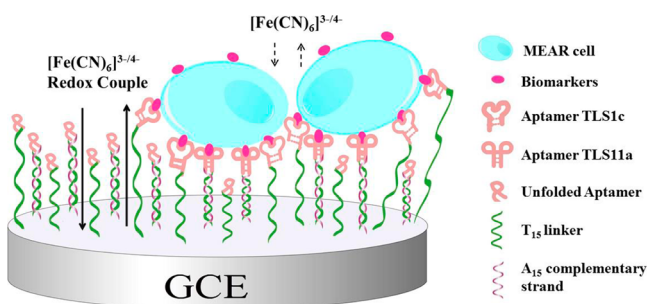
7310

dx.doi.org/10.1021/am5006783 | *ACS Appl. Mater. Interfaces* 2014, 6, 7309−7315

Figure 1. Scheme showing the designed ss-TLS1c/ds-TLS11a dual-modified electrode for specific and sensitive detection of MEAR tumor cells. In this system, two MEAR cell-specific aptamers, TLS11a and TLS1c, are conjugated to the surface of GCE via a rigid dsDNA linker (T_{15}/A_{15}) and a flexible ssDNA linker (T_{15}), respectively. Such a design could allow the most effective recognition of tumor cells by the GCE sensing surface. The specific binding of the cells to the modified electrode would bring a dramatic steric hindrance effect on the electron transfer of the redox couple $[Fe(CN)_6]^{3-/4-}$ through the GCE, while the electrostatic repulsion between negative charges of the cell surface and the $[Fe(CN)_6]^{3-/4-}$ may further inhibit the electron transfer, thus significantly reducing the electron transfer speed (see section 3.1) for a detailed description).

electron transfer of $[Fe(CN)_6]^{3-/4-}$ through the GCE, therefore introducing significant changes in the interfacial electron transfer resistance, i.e., largely reduced electron transfer speed. The electrostatic repulsion between negative charges of the cell surface and the $[Fe(CN)_6]^{3-/4-}$ redox couple may further inhibit the electron transfer through the electrode as well. Careful experiments are then carried out to demonstrate the hypothesis of our design.

3.2. Preparation and Characterization of the ss-TLS1c/ds-TLS11a Dual-Modified GCE. Before aptamer conjugation, the GCE was precleaned and oxidized to introduce carboxyl groups onto the GCE surface, providing a well-functionalized surface for further immobilization of aptamers. These functional groups were then activated by EDC and NHS, allowing their conjugation with NH_2-modified aptamers ss-TLS1c and ds-TLS11a. The oxidation and the subsequent aptamer coupling of electrode were measured by CV and EIS. The electron transfer of the redox couple $[Fe(CN)_6]^{3-/4-}$ was used as an effective indicator for electrode surface characteristics.

As shown in Figure 2A, CV of $[Fe(CN)_6]^{3-/4-}$ at the bare GCE surface possessed a couple of redox peaks with a potential difference of 90 mV. After electrochemical oxidation and dual-aptamer coupling, a significant decrease in peak current and an increase in potential difference were observed owing to the negative charges from the newly introduced DNA aptamers. To ensure detection specificity, the dual-aptamer-modified GCE was blocked in 10^9 WBC for 45 min. The blocking step resulted in a further decrease of the peak current, suggesting a certain level of nonspecific binding of WBC to the modified electrode.

The modification of GCE was also analyzed by EIS, which monitors the electrode surface by analyzing the impedance changes. In the impedance spectra, the semicircle (appeared in the high-frequency region) and the straight line (appeared in the low-frequency region) correspond to the electron transfer process and the diffusion process, respectively.[40] As shown in Figure 2B, the bare GCE displayed a nearly straight line, which is a characteristic of a mass diffusion-controlled electron transfer process.[47] Compared to bare GCE, the spectra of oxidized GCE exhibited a slight increase in the interfacial electron transfer resistance, while further coupling of the two aptamers (ss-TLS1c and ds-TLS11a) to the GCE led to an obvious increase of the charge-transfer resistance (R_{ct}), mainly due to the electrostatic repulsion between negative charges of the aptamer backbone and the $[Fe(CN)_6]^{3-/4-}$ probe. Consistent with the CV data, blocking of the dual-aptamer-modified GCE in 10^9 WBC also resulted in a significant increase in the R_{ct}, indicating that the interfacial charge-transfer was inhibited, possibly owing to the steric hindrance effect and/or negative charges contributed by the nonspecific binding of WBC to the modified electrode.

In this study, all plasma proteins in blood samples were removed due to the high background they introduced when incubated with the modified GCE, as demonstrated by the dramatic decrease of the current in CV data and the huge increase of the R_{ct} in the EIS spectra (compare the data of whole blood sample in Figure S2A,B in the Supporting Information with the 10^9 WBC data in Figure 2).

3.3. High Specificity and Excellent Sensitivity of the ss-TLS1c/ds-TLS11a Dual-Modified GCE. Specificity and sensitivity are two important features of a biosensor. We therefore investigated the specificity and sensitivity of the designed dual-aptamer-modified GCE using DPV, an extremely sensitive electrochemical detection method for trace amount
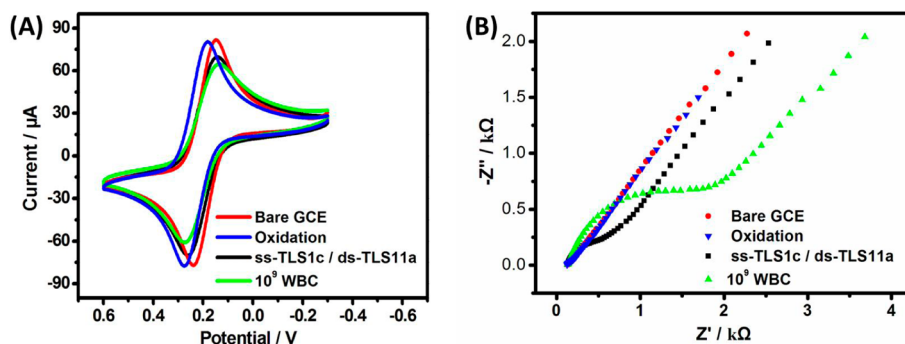

Figure 2. Characterization of the electrode after each step of surface modification by CV (A) and EIS (B) measurements: bare GCE (red), the oxidized GCE (blue), and ss-TLS1c/ds-TLS11a-modified GCE before (black) and after blocking with 1 ml PBS containing 10^9 WBC (green). All measurements were recorded in a measurement buffer containing 5 mM $[Fe(CN)_6]^{3-/4-}$ as the redox indicator. CV curves were recorded within the range of -0.3 to $+0.6$ V under a scan rate of 0.1 V/s. AC impedance spectra were recorded in the same measurement buffer in a frequency range of 0.01 Hz to 100 kHz and an AC amplitude of 0.005 V.
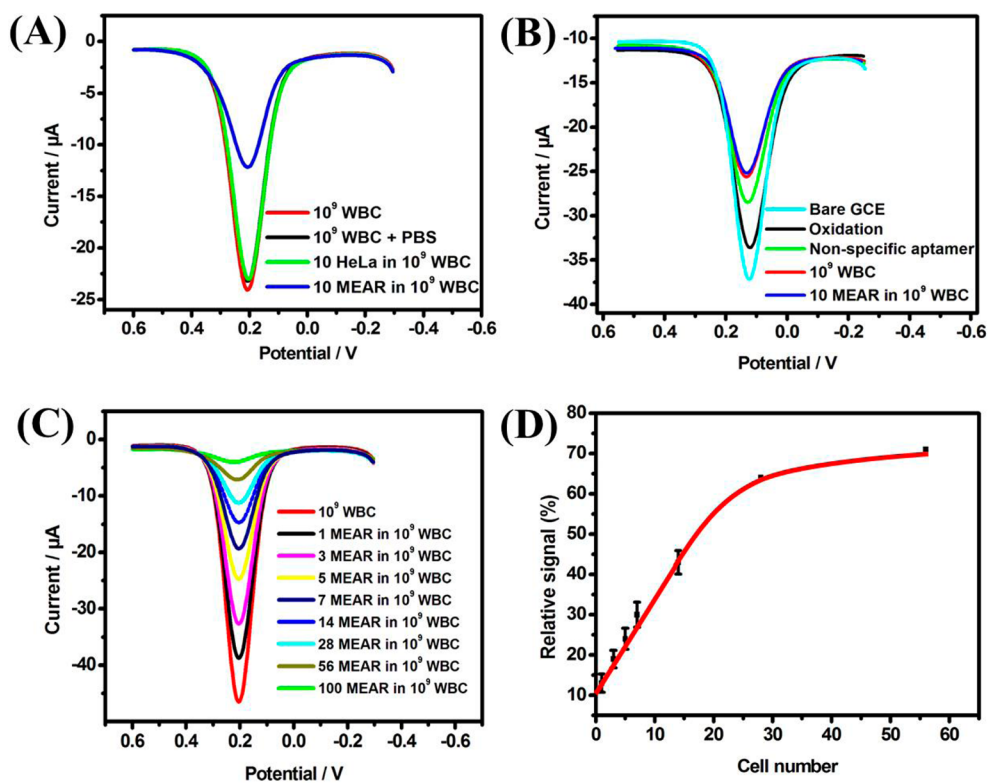
Figure 3. Highly specific and sensitive tumor cell detection using ss-TLS1c/ds-TLS11a dual-modified GCE. The modified electrodes were first blocked in 1 mL of PBS containing 10^9 WBC, and then incubated with 10^9 WBC (in 1 mL of PBS) containing indicated numbers of MEAR or HeLa cells before DPV analysis. To ensure accuracy, the exact number of cancer cells was counted under a microscope before addition into the WBC sample. (A & B) DPV measurements of different samples using ss-TLS1c/ds-TLS11a dual-modified GCE (A) and non-MEAR-specific ss-K88/ds-TBA dual-modified GCE (B): block: 1 mL of PBS containing 10^9 WBC (10^9 WBC, red line); blank, no cancer cell but PBS was added into 10^9 WBC (10^9 WBC + PBS, black line); non-specific control, 10 HeLa cells added into 10^9 WBC (10 HeLa in 10^9 WBC, green line), and 10^9 WBC containing 10 MEAR cells (10 MEAR in 10^9 WBC, blue line). (C) A representative DPV measurement of 10^9 WBC containing increasing numbers of MEAR cells (0 to 100 cells) using ss-TLS1c/ds-TLS11a dual-modified GCE. The relative signal in peak current (i) versus the number of added MEAR cells in 10^9 WBC is shown in panel D. The error bars represent relative signals across three repetitive experiments. Relative signal = (i_{sample} − i_{WBC}) / $i_{aptamer}$ × 100%.

analysis, to monitor the current decrease induced by binding of cells to immobilized aptamer probes. The redox couple $[Fe(CN)_6]^{3-/4-}$ was used as the indicator. As described above, in order to ensure the detection specificity, 10^9 WBC were used to block the aptamer-modified electrode before tumor cell detection, and the locking data were set as the basal level for all data analysis to eliminate the effect of nonspecific binding on detection. It is also worth mentioning that the WBC samples were collected from peripheral blood, washed, and resuspended in PBS to remove all free blood proteins to reduce sample complexity, which is important for sensitive detection of a low-abundant sample from a complex sample pool, such as CTC detection. Blocking of the dual-aptamer ss-TLS1c/ds-TLS11a functionalized GCE also showed a significant decrease in peak current (data not shown), consistent with the CV and EIS data (Figure 2).

After blocking, the ss-TLS1c/ds-TLS11a functionalized electrode was incubated with a desired amount of MEAR cells in 10^9 WBC to mimic the detection of cancer cells in 1 mL of peripheral blood. Excitingly, spiking of 10 MEAR cells into 10^9 WBC resulted in a huge increase in peak current of DPV compared to the blank WBC sample (Figure 3A, compare the blue line with the red line). In the marked control, when 10 HeLa cells, which should not be recognized by TLS1c and TLS11a aptamers (Figure S1 in the Supporting Information),

were added into 10^9 WBC, the electrochemical signal showed no applicable change compared to the signal obtained from WBC blocked electrode and blank sample (no tumor cell but only PBS added into 10^9 WBC) (Figure 3A, compare the green line with the red line and black line), demonstrating the high specificity of the ss-TLS1c/ds-TLS11a dual-modified electrode in tumor cell detection. The high specificity of the ss-TLS1c/ds-TLS11a dual-modified electrode was also confirmed by a control GCE dual-modified with two non-MEAR cell-specific aptamers ss-K88/ds-TBA.[41,42] These two aptamers do not recognize MEAR cells, but specifically bind *Escherichia coli* K88 strain and thrombin, respectively. No apparent change in the DPV signal was observed when the ss-K88/ds-TBA-modified GCE was incubated with 10^9 WBC or 10^9 WBC containing MEAR cells (Figure 3B).

To test the sensitivity of our designed aptamer-modified GCE, WBC samples with a series of known numbers of MEAR cells spiked were analyzed using the ss-TLS1c/ds-TLS11a dual-modified electrode. To ensure accuracy, the exact number of MEAR cells was counted under a microscope before being added into the WBC sample. As expected, ascending current peaks were observed with increasing amounts of MEAR cells in WBC samples (Figure 3C). Remarkably, as low as one MEAR cell in the 10^9 WBC could reproducibly give a detectable signal, demonstrating the extremely high sensitivity of our CTC

detection method down to the single cell level. Furthermore, a good linear relationship of the relative signal (Δsignal = (i_{sample} − i_{WBC})/$i_{aptamer}$; i: DPV peak current) versus the number of MEAR cells was observed in the range of 1 to 14 MEAR cells (Figure 3D), suggesting that our method could be a sensitive and reliable way for both detection and quantification of trace amount of specific cancer cells in peripheral blood.

3.4. Advantage of the Designed Tumor Cell Biosensing Interface. The ss-TLS1c/ds-TLS11a dual-modified electrode is able to offer excellent specificity and sensitivity in detecting trace amounts of MEAR cancer cells from WBC samples. We thus wondered whether our unique design of the biosensing interface (with dual-types of aptamers coupled to the electrode surface separately via a rigid and a flexible linker) is the key that enables such great performance in tumor cell detection. Because GCEs modified with aptamer(s) via flexible linkers (ss-TLS1c-GCE and ss-TLS1c/ss-TLS11a-GCE) showed an obvious higher background compared to the same electrodes upon subsequent converting of the surface ss-linker to ds-linker via A$_{15}$-DNA oligo incubation (Figure S3 in the Supporting Information and data not shown), two other control experiments were thus conducted. For the first one, we conjugated the two aptamers, TLS1c and TLS11a, to the GCE surface via both rigid linkers (ds-TLS1c/ds-TLS11a). For the second control, only one aptamer, TLS1c, which bound to MEAR cells more efficiently (Figure S1 in the Supporting Information), was conjugated to the electrode surface via a ds-DNA linker (ds-TLS1c). Noticeably, when the three types of electrodes, ds-TLS1c-GCE, ds-TLS1c/ds-TLS11a-GCE, and ss-TLS1c/ds-TLS11a-GCE, were used in detecting 10^9 WBC sample containing 7 MEAR cells, signals offered by ds-TLS1c-GCE and ds-TLS1c/ds-TLS11a-GCE were much lower than that obtained using the designed ss-TLS1c/ds-TLS11a-GCE (Figure 4). Again, when using the designed ss-TLS1c/ds-TLS11a electrode, we were able to detect a single MEAR cell in the WBC sample, which was impossible to be detected using either ds-TLS1c-GCE or ds-TLS1c/ds-TLS11a-GCE.

In our electrochemical CTC detection system, while pure ss-DNA would lay down on the surface of GCE due to $\pi-\pi$ stacking between the base units and the graphite surface, and

thus result in high background signals during detection, ds-DNA with paired bases would have much lower binding to the graphite surface,[48,49] and offer obviously reduced background (Figure S3 in the Supporting Information). On the other hand, on the GCE surface with mixed ds-DNA and ss-DNA, the rigid ds-DNA may be able to prevent the laying down of ss-DNA. Thus, the extended ss-DNA with a much more flexible structure compared to rigid ds-DNA may enable more efficient capture of cancer cells when they are approaching the GCE surface. Although further careful investigations are still undergoing in our laboratory to verify the above hypothesis, it is very likely that the excellent tumor cell detection sensitivity achieved using our method could indeed be attributed to our rationally designed electrode biosensing interface with aptamer conjugation via precisely controlled linkers.

3.5. Optimization of the Aptamer Density on Electrode Surface. The effect of aptamer density on the performance of the dual-modified GCE was also investigated. In addition to the electrodes used in the above experiments (0.05 nmol ss-TLS1c/0.05 nmol ds-TLS11a dual-modified GCE; GCE-0.1), two additional types of electrodes were prepared using the same protocol: GCE-0.05 (0.025 nmol ss-TLS1c/0.025 nmol ds-TLS11a dual-modified) and GCE-0.2 (0.1 nmol ss-TLS1c/0.1 nmol ds-TLS11a dual-modified). The performances of the above electrodes were then analyzed. As shown in Figure 5, compared with GCE-0.1 and GCE-0.2,

Figure 5. Effect of the aptamer density on the performance of the dual-modified GCE. Tumor cell detection was performed using three types of GCE modified with 0.025 nmol ss-TLS1c/0.025 nmol ds-TLS11a (GCE-0.05), 0.05 nmol ss-TLS1c/0.05 nmol ds-TLS11a (GCE-0.1), and 0.1 nmol ss-TLS1c/0.1 nmol ds-TLS11a (GCE-0.2), respectively. The blocking, cell binding, and DPV measurements were carried out as described in Figure 3. Error bars represent multiple measurements ($n \geq 3$). Relative sample signal = (i_{sample} − i_{WBC}) / $i_{aptamer}$. P values: * $P < 0.05$. ND: not detectable.
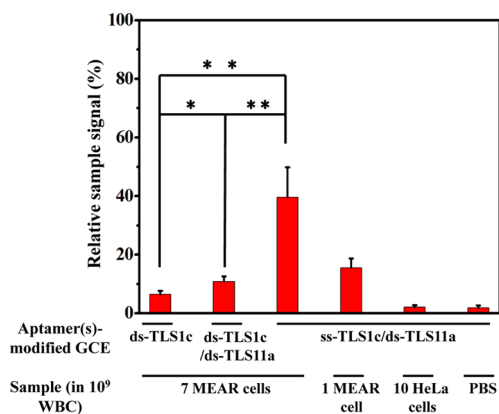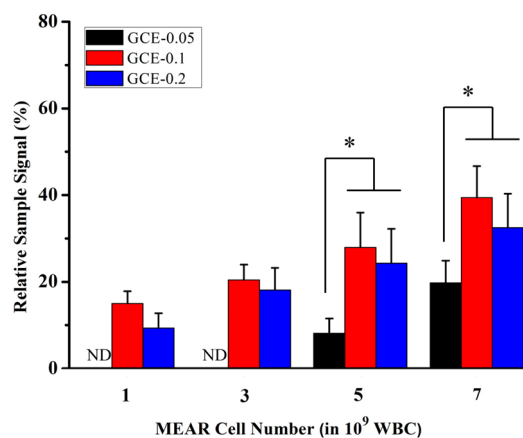
Figure 4. Comparison of tumor cell detection using three types of GCE modified with ds-TLS1c alone, ds-TLS1c/ds-TLS11a, and ss-TLS1c/ds-TLS11a, respectively. The blocking, cell binding, and DPV measurements were carried out as described in Figure 3. The electrode modified with ss-TLS1c/ds-TLS11a showed the highest signals. Error bars represent multiple measurements ($n \geq 3$). Relative sample signal = (i_{sample} − i_{WBC}) / $i_{aptamer}$. P values: * $P < 0.05$, ** $P < 0.01$.

GCE-0.05 showed largely decreased signals in all detections with a detection limit of 5 MEAR cells in 10^9 WBC, demonstrating that low aptamer density would impair the sensitivity of the electrode, likely due to insufficient probes for effective target cell capture. Increasing the total aptamer amount used to higher than 0.1 nmol did not further improve the electrode performance, suggested by the fact that GCE-0.2 and GCE-0.1 showed no significant difference in MEAR cell detection. Therefore, GCE-0.1 is considered as the cost-effective one with excellent tumor cell detection sensitivity.

4. CONCLUSION

In summary, using MEAR cells as an example, we develop a simple aptamer-based electrochemical tumor cell detection method by coupling two types of cell-specific aptamers on a commercial GCE electrode separately via a rigid and a flexible linker. The obtained ss-TLS1c/ds-TLS11a dual-modified electrode can be used for specific, sensitive, and reliable detection of tumor cells, achieving an extremely low detection limit down to single specific tumor cell in 10^9 blood cells. By comparing with several control GCEs, the results demonstrate the advantages of our rationally designed electrode in tumor cell sensing, and suggest the importance in the careful design of nano−bio interfaces to optimize the performance of biosensors in general. Moreover, the aptamer-based electrochemical method presented in our work is an easy and rapid detection approach, which could be particularly suitable for sensitive and timely detection of trace amounts of cancer cells in peripheral blood and may hold great potential in early diagnosis or sensitive prognosis of tumor development and metastasis.

ASSOCIATED CONTENT

Ⓢ Supporting Information

Additional information about the specific recognition of TLS1c and TLS11a to MEAR cells analyzed using flow cytometry assay, the effect of plasma proteins on tumor cell detection, and the effect of converting the ss-linker to ds-linker on the interfacial electron transfer to the electrode surface. This material is available free of charge via the Internet at http://pubs.acs.org.

AUTHOR INFORMATION

Corresponding Authors
*R. Peng. Tel: +86-0512-65880947. Fax: +86-0512-65880820. E-mail: rpeng@suda.edu.cn.
*L.G. Xu. Tel: +86-0512-65880927. Fax: +86-0512-65880820. E-mail: lgxu@suda.edu.cn.

Notes
The authors declare no competing financial interest.

ACKNOWLEDGMENTS

REFERENCES

(1) Joosse, S. A.; Pantel, K. Biologic Challenges in the Detection of Circulating Tumor Cells. *Cancer Res.* **2013**, *73*, 8−11.

(2) Pantel, K.; Alix-Panabières, C. Circulating Tumour Cells in Cancer Patients: Challenges and Perspectives. *Trends Mol. Med.* **2010**, *16*, 398−406.

(3) Gerges, N.; Rak, J.; Jabado, N. New Technologies for the Detection of Circulating Tumour Cells. *Br. Med. Bull.* **2010**, *94*, 49−64.

(4) Paterlini-Brechot, P.; Benali, N. L. Circulating Tumor Cells (Ctc) Detection: Clinical Impact and Future Directions. *Cancer Lett.* **2007**, *253*, 180−204.

(5) Hou, S.; Zhao, H.; Zhao, L.; Shen, Q.; Wei, K. S.; Suh, D. Y.; Nakao, A.; Garcia, M. A.; Song, M.; Lee, T. Capture and Stimulated Release of Circulating Tumor Cells on Polymer-Grafted Silicon Nanostructures. *Adv. Mater.* **2012**, *25*, 1547−1551.

(6) Balzar, M.; Winter, M.; De Boer, C.; Litvinov, S. The Biology of the 17−1a Antigen (Ep-Cam). *J. Mol. Med.* **1999**, *77*, 699−712.

(7) Nagrath, S.; Sequist, L. V.; Maheswaran, S.; Bell, D. W.; Irimia, D.; Ulkus, L.; Smith, M. R.; Kwak, E. L.; Digumarthy, S.; Muzikansky, A. Isolation of Rare Circulating Tumour Cells in Cancer Patients by Microchip Technology. *Nature* **2007**, *450*, 1235−1239.

(8) Allard, W. J.; Matera, J.; Miller, M. C.; Repollet, M.; Connelly, M. C.; Rao, C.; Tibbe, A. G.; Uhr, J. W.; Terstappen, L. W. Tumor Cells Circulate in the Peripheral Blood of All Major Carcinomas but Not in Healthy Subjects or Patients with Nonmalignant Diseases. *Clin. Cancer Res.* **2004**, *10*, 6897−6904.

(9) Cruz, I.; Cruz, J. J.; Ramos, M.; Gómez-Alonso, A.; Adansa, J. C.; Rodríguez, C.; Orfao, A. Evaluation of Multiparameter Flow Cytometry for the Detection of Breast Cancer Tumor Cells in Blood Samples. *Am. J. Clin. Pathol.* **2005**, *123*, 66−74.

(10) Iakovlev, V. V.; Goswami, R. S.; Vecchiarelli, J.; Arneson, N. C.; Done, S. J. Quantitative Detection of Circulating Epithelial Cells by Q-Rt-Pcr. *Breast Cancer Res. Treat.* **2008**, *107*, 145−154.

(11) Mostert, B.; Sleijfer, S.; Foekens, J. A.; Gratama, J. W. Circulating Tumor Cells (Ctcs): Detection Methods and Their Clinical Relevance in Breast Cancer. *Cancer Treat. Rev.* **2009**, *35*, 463−474.

(12) Wang, J.; Qu, X. Recent Progress in Nanosensors for Sensitive Detection of Biomolecules. *Nanoscale* **2013**, *5*, 3589−3600.

(13) He, L.; Liu, Y.; Liu, J.; Xiong, Y.; Zheng, J.; Liu, Y.; Tang, Z. Core−Shell Noble-Metal@ Metal-Organic-Framework Nanoparticles with Highly Selective Sensing Property. *Angew. Chem., Int. Ed.* **2013**, *52*, 3741−3745.

(14) Yin, S.; Wu, Y. L.; Hu, B.; Wang, Y.; Cai, P.; Tan, C. K.; Qi, D.; Zheng, L.; Leow, W. R.; Tan, N. S. Three-Dimensional Graphene Composite Macroscopic Structures for Capture of Cancer Cells. *Adv. Mater. Interfaces* **2014**, *1*, 1300043.

(15) Feng, L.; Chen, Y.; Ren, J.; Qu, X. A Graphene Functionalized Electrochemical Aptasensor for Selective Label-Free Detection of Cancer Cells. *Biomaterials* **2011**, *32*, 2930−2937.

(16) Xu, J.-J.; Zhao, W.-W.; Song, S.; Fan, C.; Chen, H.-Y. Functional Nanoprobes for Ultrasensitive Detection of Biomolecules: An Update. *Chem. Soc. Rev.* **2014**, *43*, 1601−1611.

(17) Jiang, Y.; Meng, F.; Qi, D.; Cai, P.; Yin, Z.; Shao, F.; Zhang, H.; Boey, F.; Chen, X. Gold Nanotip Array for Ultrasensitive Electrochemical Sensing and Spectroscopic Monitoring. *Small* **2013**, *9*, 2260−2265.

(18) Wu, Y.; Xue, P.; Kang, Y.; Hui, K. M. Highly Specific and Ultrasensitive Graphene-Enhanced Electrochemical Detection of Low-Abundance Tumor Cells Using Silica Nanoparticles Coated with Antibody-Conjugated Quantum Dots. *Anal. Chem.* **2013**, *85*, 3166−3173.

(19) Ellington, A. D.; Szostak, J. W. In Vitro Selection of Rna Molecules That Bind Specific Ligands. *Nature* **1990**, *346*, 818−822.

(20) Tuerk, C.; Gold, L. Systematic Evolution of Ligands by Exponential Enrichment: Rna Ligands to Bacteriophage T4 DNA Polymerase. *Science* **1990**, *249*, 505−510.

(21) Wu, C.; Han, D.; Chen, T.; Peng, L.; Zhu, G.; You, M.; Qiu, L.; Sefah, K.; Zhang, X.-B.; Tan, W. Building a Multifunctional Aptamer-Based DNA Nanoassembly for Targeted Cancer Therapy. *J. Am. Chem. Soc.* **2013**, *135*, 18644−18650.

(22) Zhang, J.; Wang, L.; Zhang, H.; Boey, F.; Song, S.; Fan, C. Aptamer-Based Multicolor Fluorescent Gold Nanoprobes for Multiplex Detection in Homogeneous Solution. *Small* **2010**, *6*, 201−204.

(23) Tan, W.; Donovan, M. J.; Jiang, J. Aptamers from Cell-Based Selection for Bioanalytical Applications. *Chem. Rev.* **2013**, *113*, 2842−2862.

(24) Xia, F.; White, R. J.; Zuo, X.; Patterson, A.; Xiao, Y.; Kang, D.; Gong, X.; Plaxco, K. W.; Heeger, A. J. An Electrochemical Supersandwich Assay for Sensitive and Selective DNA Detection in Complex Matrices. *J. Am. Chem. Soc.* **2010**, *132*, 14346−14348.

(25) Dave, N.; Liu, J. Biomimetic Sensing Based on Chemically Induced Assembly of a Signaling DNA Aptamer on a Fluid Bilayer Membrane. *Chem. Commun.* **2012**, *48*, 3718−3720.

(26) Li, J.; Xu, M.; Huang, H.; Zhou, J.; Abdel-Halimb, E.; Zhang, J.-R.; Zhu, J.-J. Aptamer-Quantum Dots Conjugates-Based Ultrasensitive Competitive Electrochemical Cytosensor for the Detection of Tumor Cell. *Talanta* **2011**, *85*, 2113−2120.

(27) KangáKu, J. Simultaneous Electrochemical Detection of Both Psma (+) and Psma (−) Prostate Cancer Cells Using an Rna/Peptide Dual-Aptamer Probe. *Chem. Commun.* **2010**, *46*, 5566−5568.

(28) Huang, P.-J. J.; Liu, J. Flow Cytometry-Assisted Detection of Adenosine in Serum with an Immobilized Aptamer Sensor. *Anal. Chem.* **2010**, *82*, 4020−4026.

(29) Zuo, X.; Song, S.; Zhang, J.; Pan, D.; Wang, L.; Fan, C. A Target-Responsive Electrochemical Aptamer Switch (Treas) for Reagentless Detection of Nanomolar Atp. *J. Am. Chem. Soc.* **2007**, *129*, 1042−1043.

(30) Liu, J.; Zhou, H.; Xu, J.-J.; Chen, H.-Y. An Effective DNA-Based Electrochemical Switch for Reagentless Detection of Living Cells. *Chem. Commun.* **2011**, *47*, 4388−4390.

(31) Cai, L.; Chen, Z.-Z.; Chen, M.-Y.; Tang, H.-W.; Pang, D.-W. Muc-1 Aptamer-Conjugated Dye-Doped Silica Nanoparticles for Mcf-7 Cells Detection. *Biomaterials* **2012**, *34*, 371−381.

(32) He, Y.; Wang, Z.-G.; Tang, H.-W.; Pang, D.-W. Low Background Signal Platform for the Detection of Atp: When a Molecular Aptamer Beacon Meets Graphene Oxide. *Biosens. Bioelectron.* **2011**, *29*, 76−81.

(33) Kong, R. M.; Zhang, X. B.; Chen, Z.; Tan, W. Aptamer-Assembled Nanomaterials for Biosensing and Biomedical Applications. *Small* **2011**, *7*, 2428−2436.

(34) Liu, Y.; Dong, X.; Chen, P. Biological and Chemical Sensors Based on Graphene Materials. *Chem. Soc. Rev.* **2012**, *41*, 2283−2307.

(35) Feng, L.; Wu, L.; Qu, X. New Horizons for Diagnostics and Therapeutic Applications of Graphene and Graphene Oxide. *Adv. Mater.* **2013**, *25*, 168−186.

(36) Wu, L.; Wang, J.; Yin, M.; Ren, J.; Miyoshi, D.; Sugimoto, N.; Qu, X. Reduced Graphene Oxide Upconversion Nanoparticle Hybrid for Electrochemiluminescent Sensing of a Prognostic Indicator in Early-Stage Cancer. *Small* **2013**, *10*, 330−336.

(37) Wu, L.; Wang, J.; Ren, J.; Qu, X. Ultrasensitive Telomerase Activity Detection in Circulating Tumor Cells Based on DNA Metallization and Sharp Solid-State Electrochemical Techniques. *Adv. Funct. Mater.* **2014**, DOI: 10.1002/adfm.201303818.

(38) Zhong, H.; Zhang, Q.; Zhang, S. High-Intensity Fluorescence Imaging and Sensitive Electrochemical Detection of Cancer Cells by Using an Extracellular Supramolecular Reticular DNA-Quantum Dot Sheath. *Chem.—Eur. J.* **2011**, *17*, 8388−8394.

(39) Pan, C.; Guo, M.; Nie, Z.; Xiao, X.; Yao, S. Aptamer-Based Electrochemical Sensor for Label-Free Recognition and Detection of Cancer Cells. *Electroanalysis* **2009**, *21*, 1321−1326.

(40) Shangguan, D.; Meng, L.; Cao, Z. C.; Xiao, Z.; Fang, X.; Li, Y.; Cardona, D.; Witek, R. P.; Liu, C.; Tan, W. Identification of Liver Cancer-Specific Aptamers Using Whole Live Cells. *Anal. Chem.* **2008**, *80*, 721−728.

(41) Li, H.; Ding, X.; Peng, Z.; Deng, L.; Wang, D.; Chen, H.; He, Q. Aptamer Selection for the Detection of Escherichia Coli K88. *Can. J. Microbiol.* **2011**, *57*, 453−459.

(42) Macaya, R. F.; Schultze, P.; Smith, F. W.; Roe, J. A.; Feigon, J. Thrombin-Binding DNA Aptamer Forms a Unimolecular Quadruplex Structure in Solution. *Proc. Natl. Acad. Sci. U. S. A.* **1993**, *90*, 3745−3749.

(43) Xu, J.; He, X.; Jin, L.; Jiang, L.; Zhou, Y.; Kang, Z.; Peng, R.; Lee, S.-T. A Protein-Based Electrochemical Method for Label-Free Characterization of Sequence-Specific Protein−DNA Interactions. *Electrochim. Acta* **2011**, *56*, 5759−5765.

(44) Xu, G.; Jiao, K.; Fan, J.; Sun, W. Electrochemical Detection of Specific Gene Related to Camv35s Using Methylene Blue and Ethylenediamine-Modified Glassy Carbon Electrode. *Acta Chim. Slov.* **2006**, *53*, 486.

(45) Vettore, L.; De Matteis, M. C.; Zampini, P. A New Density Gradient System for the Separation of Human Red Blood Cells. *Am. J. Hematol.* **1980**, *8*, 291−297.

(46) Pei, H.; Lu, N.; Wen, Y.; Song, S.; Liu, Y.; Yan, H.; Fan, C. A DNA Nanostructure-Based Biomolecular Probe Carrier Platform for Electrochemical Biosensing. *Adv. Mater.* **2010**, *22*, 4754−4758.

(47) Li, G.; Li, X.; Wan, J.; Zhang, S. Dendrimers-Based DNA Biosensors for Highly Sensitive Electrochemical Detection of DNA Hybridization Using Reporter Probe DNA Modified with Au Nanoparticles. *Biosens. Bioelectron.* **2009**, *24*, 3281−3287.

(48) Dong, X.; Shi, Y.; Huang, W.; Chen, P.; Li, L. J. Electrical Detection of DNA Hybridization with Single-Base Specificity Using Transistors Based on Cvd-Grown Graphene Sheets. *Adv. Mater.* **2010**, *22*, 1649−1653.

(49) He, S.; Song, B.; Li, D.; Zhu, C.; Qi, W.; Wen, Y.; Wang, L.; Song, S.; Fang, H.; Fan, C. A Graphene Nanoprobe for Rapid, Sensitive, and Multicolor Fluorescent DNA Analysis. *Adv. Funct. Mater.* **2010**, *20*, 453−459.